

Supporting Information

Ultrathin Cu₂O as an efficient inorganic hole transporting material for perovskite solar cells

Weili Yu, Feng Li, Hong Wang, Erkki Alarousu, Yin Chen, Bin Lin, Lingfei Wang, Mohamed Nejib Hedhili, Yangyang Li, Kewei Wu, Xianbin Wang, Omar F. Mohammed, and Tom Wu

HTM	Method	Device Structure	Work function [eV]	V _{oc} [V]	J _{sc} [mA/cm ²]	FF [%]	PCE [%]	Ref.
CuSCN	Doctor blading	Mesoporous	5.3	1.02	19.70	62.0	12.4	1
CuSCN	Electrodeposition	Planar	—	1.0	21.9	75.8	16.6	2
CuI	Drop-casting	Mesoporous	5.2 ^{a)}	0.55	17.80	62.0	6.0	3
NiO	Spin-coating	Planar	5.36	0.88	16.27	63.5	9.1	4
NiO	Spin-coating	Planar	5.4	0.92	12.43	68	7.8	5
NiO	Spin-coating	Planar	5.26	1.05	15.4	48	7.6	6
NiO	Spin-coating	Mesoporous	5.2 ^{a)}	1	14.65	64	9.44	7
NiO	Screen-printing	Mesoporous	5.1 ^{a)}	0.83	4.9	35	1.5	8
NiO	Electrodeposition	Planar	5.4 ^{a)}	0.786	14.2	65	7.26	9
NiOx	Sputter	Mesoporous	—	0.96	19.8	61	11.6	10
Cu (5 at%) doped NiO	Spin-coating	Planar	—	1.11	18.75	72	14.98	11
Cu ₂ O	Chemical reaction	Planar	5.2 ^{a)}	1.07	16.52	75.51	13.35	12
Cu ₂ O	Sputter	Planar	4.84	0.95	17.50	66.2	11.0	This work

Table S1. State of art researches on inorganic HTMs reported in perovskite solar cells.

^{a)} Valence band value was provided instead of work function.

Table S2. The prices of commercial organic HTMs, in comparison with Cu₂O.

HTMs	Catalog #	Price (EUR) ^{a)}
Spiro-MeOTAD	792071-1G	331
PEDOT:PSS	483095-250G (1.3 wt%)	211.5
PTAA	702471-100MG	422
P3HT	445703-1G	565
Cu ₂ O	566284-5G	51.6

^{a)} All data in this table is from Sigma-Aldrich website on 10/5/2015.

Table S3. Transient absorption characteristics of perovskite layers on different substrates.

Samples	τ_1		τ_2	
	Lifetime (ns)	Content (%)	Lifetime (ns)	Content (%)
PS/glass	5.51±0.3	77	22.83±2.87	23
PS/Cu ₂ O/glass	3.88±0.27	47	33.40±1.33	53
PS/PEDOT:PSS/glass	9.11±0.99	39	40.06±2.67	61

The kinetic spectrum was fitted according to the double exponential function:

$$y = y_0 + A_1 \exp\left(-\frac{t}{\tau_1}\right) + A_2 \exp\left(-\frac{t}{\tau_2}\right)$$

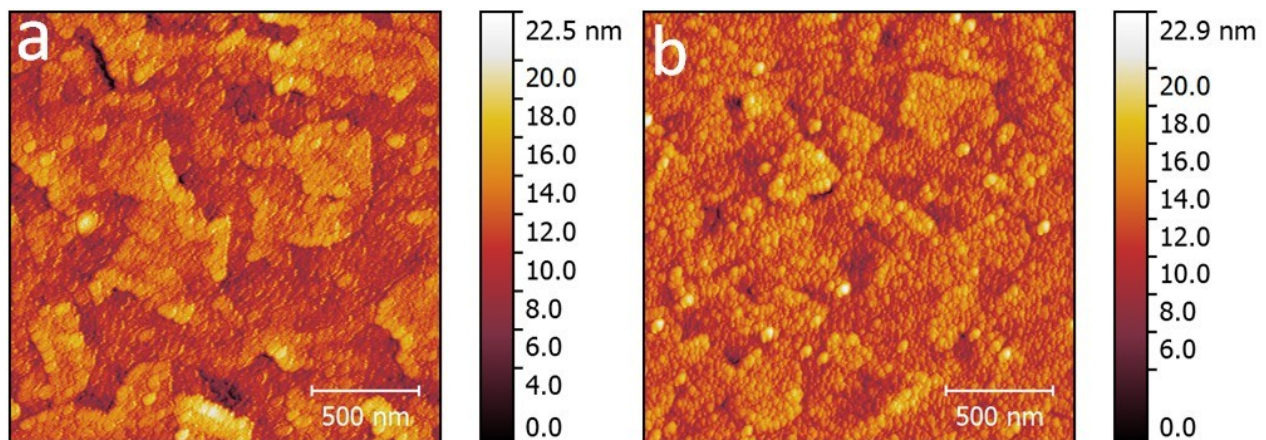


Figure S1. AFM image of a) ITO and b) 5 nm Cu₂O film covered ITO glass slide. The AFM indicates that the Cu₂O layer on ITO glass is uniform and the grain size is narrowly distributed. Average grain size: 40 nm.

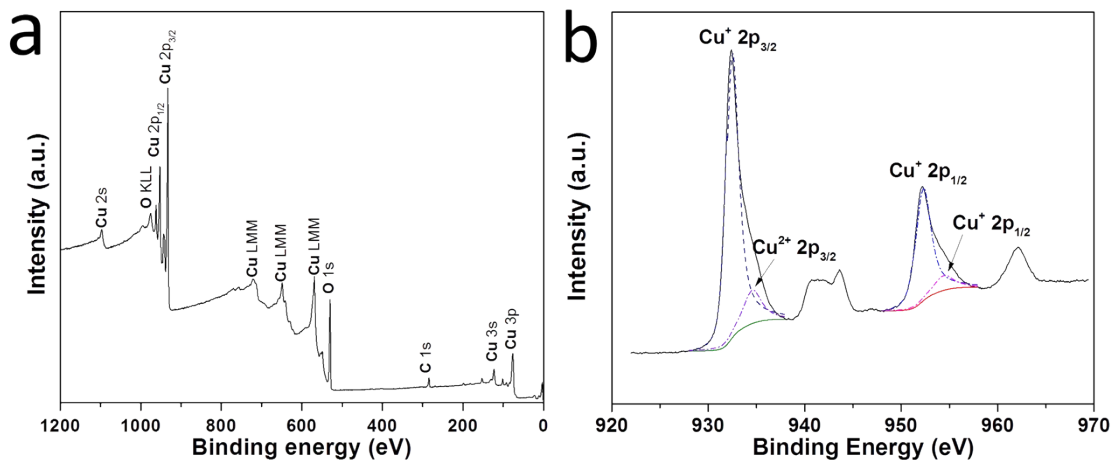


Figure S2. a) XPS survey spectrum and b) high resolution XPS spectrum of Cu 2p core level. From survey spectrum a), Cu, O, C elements are detected. The Cu 2p_{3/2} core peak (928 eV – 937 eV) is fitted using two components located at 932.4 eV and 934.6 eV, corresponding to Cu¹⁺ and Cu²⁺ with the atomic percent of 86% and 14%, respectively.^{13,14}

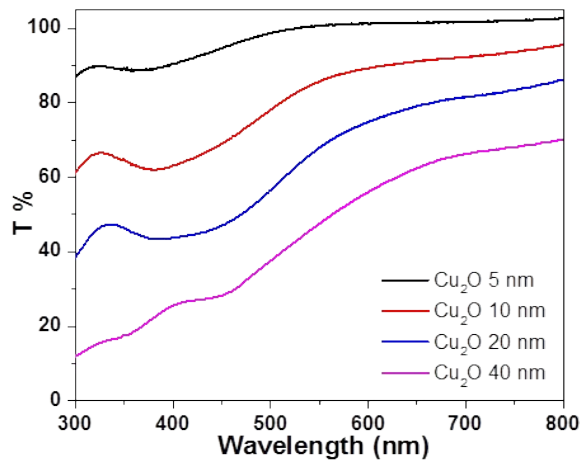


Figure S3. The transmittance spectra of Cu_2O layer with different thickness on ITO glass. The dependence of transmittance indicates that the Cu_2O layer has high absorption coefficient, which matches well with the data we presented in Figure 1 d). To confirm that most of incident light be absorbed by the perovskite layer, 5 nm thickness of Cu_2O layer was chosen to fabricate solar cells.

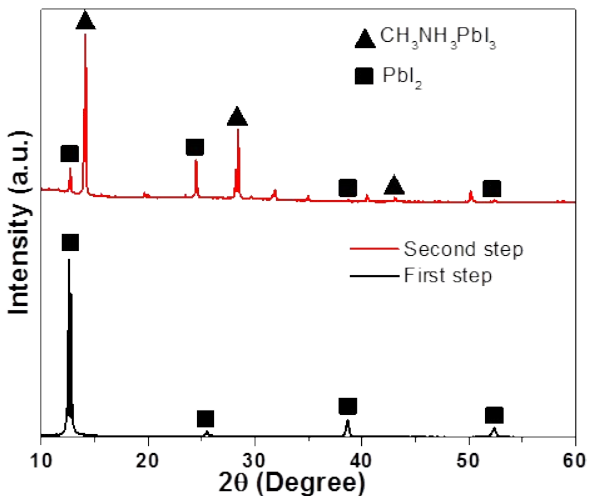


Figure S4. XRD of PbI_2 and perovskite prepared by the two-step process. The XRD spectra indicate that besides $\text{CH}_3\text{NH}_3\text{PbI}_3$, there is still some PbI_2 left after dipping into $\text{CH}_3\text{NH}_3\text{I}$ solution for 30 s. This spectrum is consistent with previous report that the $\text{CH}_3\text{NH}_3\text{I}$ insertion hardly proceeds beyond the surface of thin PbI_2 films, and that the complete transformation of the crystal structure requires several hours and the perovskite dissolves in the $\text{CH}_3\text{NH}_3\text{I}$ solution, hampering the transformation.¹⁵ However, the incomplete conversion seemed to work as we still got high efficiencies with the same method utilized in some references.^{16, 17} The reason is the passivation effect of PbI_2 , which acts as a blocking layer between Cu_2O and the perovskite itself, reducing the probability of back electron transfer (charge recombination).¹⁸

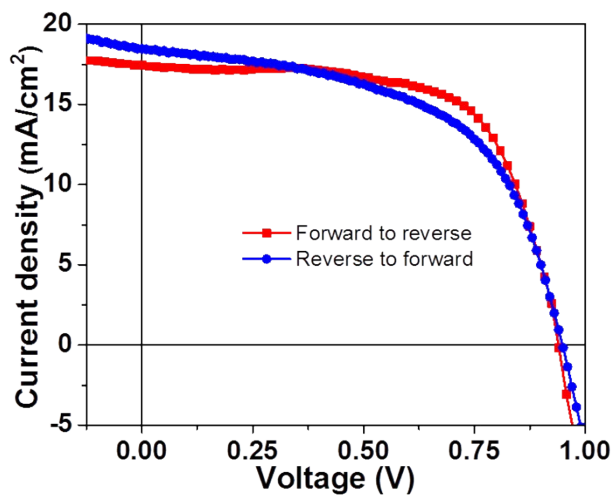


Figure S5. Hysteresis of $\text{CH}_3\text{NH}_3\text{PbI}_3$ perovskite solar cells using 5 nm Cu_2O as HTM.

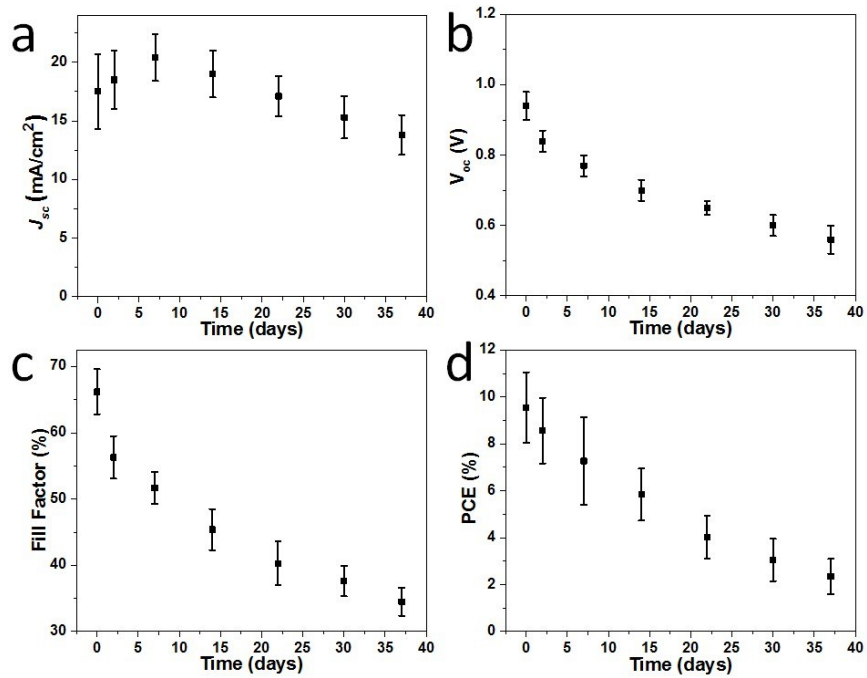


Figure S6. Stability of $\text{CH}_3\text{NH}_3\text{PbI}_3$ perovskite solar cell with 5 nm Cu_2O layer as HTM. The decrease of solar cells PCE is mainly attributed to the decrease of V_{oc} and FF, which is most probably caused by the oxidation of Ag electrode and the Cu_2O layer due to the penetration of oxygen.

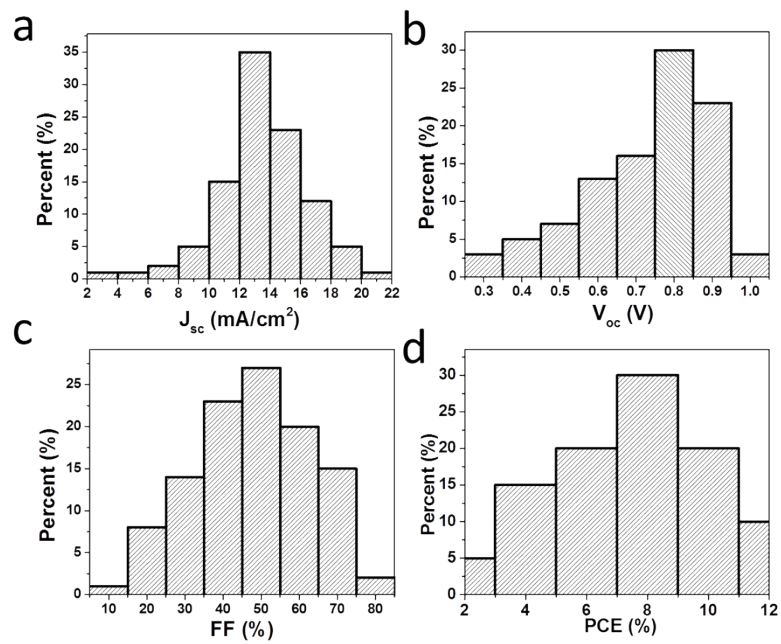


Figure S7. The statistical histogram plots of J_{sc} , V_{oc} , FF and PCE for perovskite solar cells based on 5 nm Cu_2O HTM.

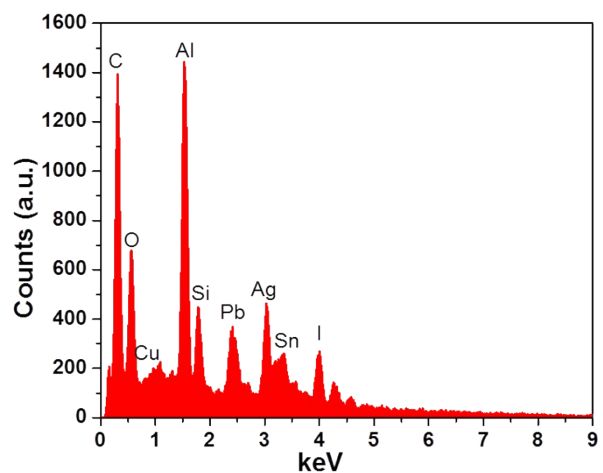


Figure S8. The EDAX spectrum of ITO/Cu₂O/CH₃NH₃PbI₃ solar cells.

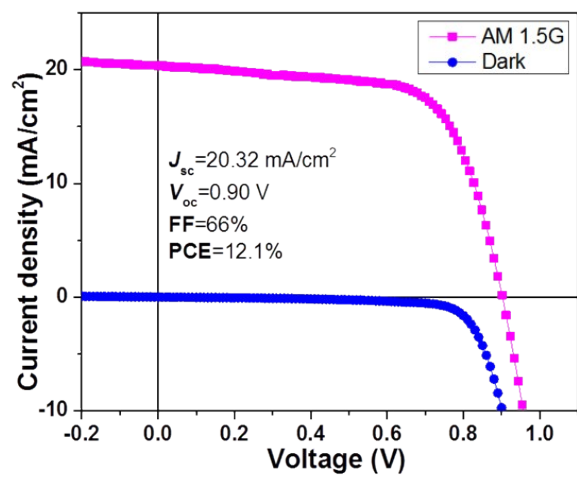


Figure S9. The I-V performance of solar cells based on glass/ITO/PEDOT:PSS substrate.

References

1. P. Qin, S. Tanaka, S. Ito, N. Tetraeault, K. Manabe, H. Nishino, M. K. Nazeeruddin, M. Graetzel, *Nat. Commun.*, 2014, **5**, 3834.
2. S. Ye, W. Sun, Y. Li, W. Yan, H. Peng, Z. Bian, Z. Liu, C. Huang, *Nano Lett.*, 2015, **15**, 3723.
3. J. A. Christians, R. C. M. Fung, P. V. Kamat, *J. Am. Chem. Soc.*, 2004, **136**, 758.
4. Z. Zhu, Y. Bai, T. Zhang, Z. Liu, X. Long, Z. Wei, Z. Wang, L. Zhang, J. Wang, F. Yan, S. Yang, *Angew. Chem. Int. Ed.*, 2014, **53**, 12571.
5. J. Y. Jeng, K. C. Chen, T. Y. Chiang, P. Y. Lin, T. D. Tsai, Y. C. Chang, T. F. Guo, P. Chen, T. C. Wen, Y. J. Hsu, *Adv. Mater.*, 2014, **26**, 4107.
6. L. Hu, J. Peng, W. W. Wang, Z. Xia, J. Y. Yuan, J. L. Lu, X. D. Huang, W. L. Ma, H. B. Song, W. Chen, Y. B. Cheng, J. Tang, *ACS Photon.* 2014, **1**, 547.
7. K.-C. Wang, J.-Y. Jeng, P.-S. Shen, Y.-C. Chang, E. W.-G. Diau, C.-H. Tsai, T.-Y. Chao, H.-C. Hsu, P.-Y. Lin, P. Chen, T.-F. Guo, T.-C. Wen, *Sci. Rep.*, 2014, **4**, 4756.
8. H. N. Tian, B. Xu, H. Chen, E. M. J. Johansson, G. Boschloo, *ChemSusChem*, 2014, **7**, 2150.
9. A. S. Subbiah, A. Halder, S. Ghosh, N. Mahuli, G. Hodes, S. K. Sarkar, *J. Phys. Chem. Lett.*, 2014, **5**, 1748.
10. K. C. Wang, P. S. Shen, M. H. Li, S. Chen, M. W. Lin, P. Chen, T. F. Guo, *ACS Appl. Mater. Interfaces*, 2014, **6**, 11851.
11. J. H. Kim, P.-W. Liang, S. T. Williams, N. Cho, C.-C. Chueh, M. S. Glaz, D. S. Ginger, A. K. Y. Jen, *Adv. Mater.*, 2015, **27**, 695.
12. C. Zuo, L. Ding, *Small* 2015, DOI: 10.1002/smll.201501330.
13. M.C. Biesinger, *Appl. Surf. Sci.* 2010, **257**, 887.
14. L. Martin, *J. Phys. Chem. C* 2013, **117**, 4421.
15. J. Burschka, N. Pellet, S.-J. Moon, R. Humphry-Baker, P. Gao, M. K. Nazeeruddin, M. Graetzel, *Nature*, 2013, **499**, 316.
16. D. Liu, T. L. Kelly, *Nat. Photon.*, 2014, **8**, 133.
17. J.-H. Im, I.-H. Jang, N. Pellet, M. Graetzel, N.-G. Park, *Nat. Nanotechnol.*, 2014, **9**, 927.
18. D. H. Cao, C. C. Stoumpos, C. D. Malliakas, M. J. Katz, O. K. Farha, J. T. Hupp, M. G. Kanatzidis, *APL Mater.*, 2014, **2**, 091101.